



Empirical determinants of measles metapopulation dynamics in England and Wales

Bärbel Finkenstädt and Bryan Grenfell

Department of Zoology, University of Cambridge, Cambridge CB2 3EJ, UK

A key issue in metapopulation dynamics is the relative impact of internal patch dynamics and coupling between patches. This problem can be addressed by analysing large spatiotemporal data sets, recording the local and global dynamics of metapopulations. In this paper, we analyse the dynamics of measles metapopulations in a large spatiotemporal case notification data set, collected during the pre-vaccination era in England and Wales. Specifically, we use generalized linear statistical models to quantify the relative importance of local influences (birth rate and population size) and regional coupling on local epidemic dynamics. Apart from the proportional effect of local population size on case totals, the models indicate patterns of local and regional dynamic influences which depend on the current state of epidemics. Birth rate and geographic coupling are not associated with the size of major epidemics. By contrast, minor epidemics—and especially the incidence of local extinction of infection—are influenced both by birth rate and geographical coupling. Birth rate at a lag of four years provides the best fit, reflecting the delayed recruitment of susceptibles to school cohorts. A hierarchical index of spatial coupling to large centres provides the best spatial model. The model also indicates that minor epidemics and extinction patterns are more strongly influenced by this regional effect than the local impact of birth rate.

Keywords: statistical population dynamics; measles; birth rate; spatial diffusion; fadeout pattern; generalized linear models

1. INTRODUCTION

What is the relative influence of local and regional effects on the spatiotemporal dynamics of populations? This question has been a major recurring theme in ecology. The greatest development of relevant theoretical and empirical work has been under the banner of metapopulation studies. Metapopulation theory has focused mainly on the role of low level coupling in promoting the persistence of populations (Levins 1969; Gilpin & Hanski 1991; Hassell *et al.* 1991; Allen *et al.* 1993; Holt 1994; Ruxton 1994; Grenfell *et al.* 1995b; Hanski *et al.* 1996; Sutcliffe *et al.* 1997b). Understanding the balance between local and global dynamics is a central issue here, and a number of theoretical and empirical studies have recently addressed this question (Hanski *et al.* 1995; Bjørnstad *et al.* 1995, 1996; Hill *et al.* 1996; Kuussaari *et al.* 1996; Sutcliffe *et al.* 1996, 1997b; Ranta *et al.* 1997). We can distinguish a continuum of spatial interaction strength: from completely separate local populations, via weakly coupled metapopulations, to globally interacting populations made up of strongly coupled patches (Sutcliffe *et al.* 1997a).

In order to quantify the balance between local and global dynamics, we ideally require large spatiotemporal data sets for the population in question. Such data sets are rare in ecology. This contrasts with the study of some human microparasitic infections, where disease notification schemes have led to large historical records of the incidence of infection (Anderson & May 1991), along with a mass of relevant demographic data. Measles is the paradigm—large, relatively reliable data sets, simple natural

history and public health significance have led to a large body of epidemiological research on the spatiotemporal dynamics of measles infection (Bartlett 1957, 1960; May & Anderson 1984; Dietz & Schenzle 1985; Anderson & May 1991; Cliff *et al.* 1993; Grenfell *et al.* 1995c; Bolker & Grenfell 1995, 1996; Ferguson *et al.* 1997; Keeling & Grenfell 1997). Ecological studies of measles have concentrated mainly on the question of nonlinear dynamics and chaos (Schaffer & Kot 1985; Olsen *et al.* 1988; Grenfell 1992; Grenfell *et al.* 1994b). However, there are also deep analogies between the spatial dynamics of measles epidemics and the metapopulation concept (Lawton *et al.* 1994; Nee 1994; Grenfell & Harwood 1997). As with metapopulation studies, determinants of population extinction (here of the infectious agent) have been a major preoccupation in epidemiology. The seminal contribution here is Bartlett's characterization of the critical community size (CCS)—a stochastic host population threshold of 300 000–500 000 individuals above which infection tended to persist through epidemic troughs before the vaccine era. Below this population size, infection frequently experienced 'fadeout' (local extinction) in the troughs between major epidemics, with subsequent reintroduction of infection from other parts of the disease metapopulation.

This paper analyses the spatiotemporal dynamics of measles epidemics in England and Wales. We use a large epidemiological and demographic database to characterize the pattern of local epidemics in terms of a balance between local factors (birth rate and population size) and regional factors (coupling to other centres). Measles epidemics are fuelled by recruitment of susceptible

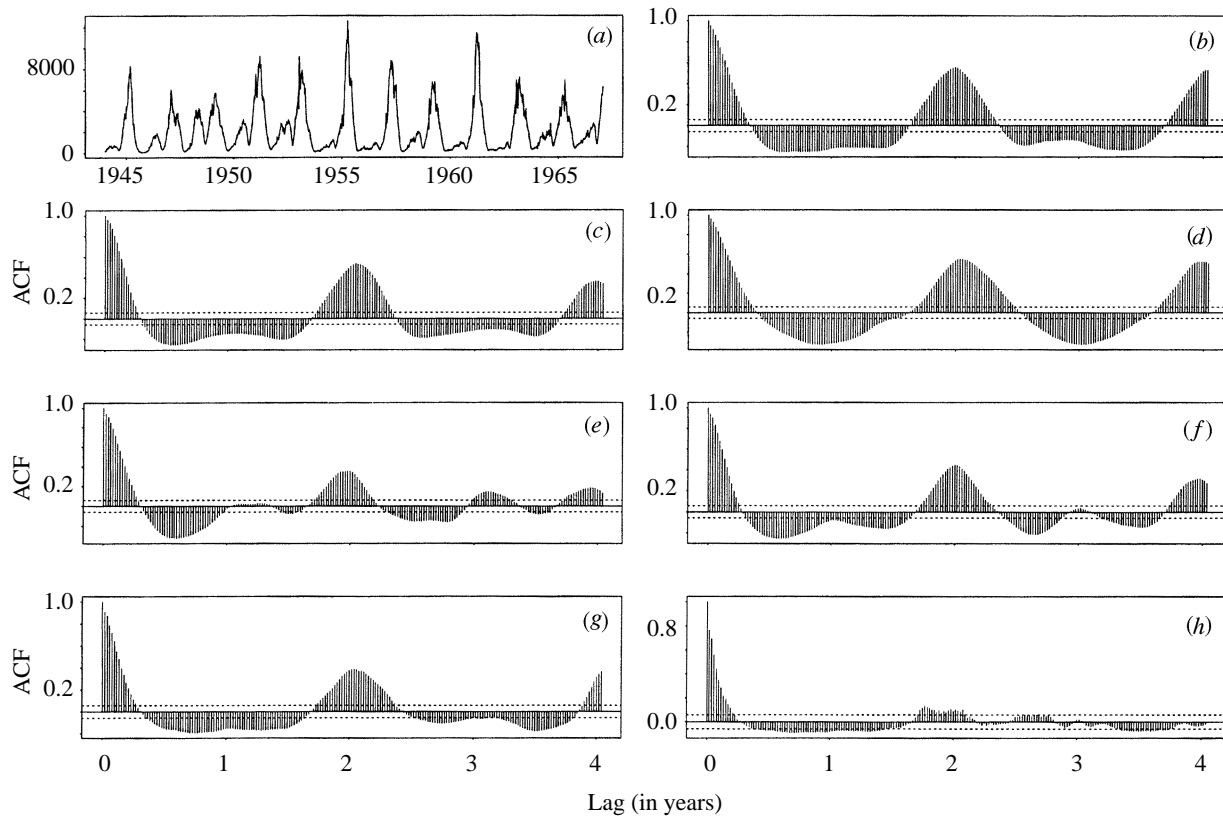


Figure 1. (a) Time series plot of the measles notifications for the total sum of 60 cities during the pre-vaccination era from 1944 to 1966. (b)–(h) Autocorrelation function (ACF) for a sample of selected cities for a lag of up to four years. Horizontal bands are 95% confidence limits for a zero correlation. London (b), Birmingham (c), Manchester (d), and Norwich (g) have a clear biennial cyclicity. Liverpool (e) and Coventry (f) have mixtures between annual and biennial cyclicity. King's Lynn (h) and other small towns have a more irregular pattern of the ACF.

individuals, generated ultimately by births. Birth rate and population size therefore provide readily available measures of dynamically relevant local characteristics. The next section introduces the data set and describes basic epidemic patterns. We then outline the statistical approach—a cross-sectional study, based on generalized linear models (GLMs). After describing the results of the analysis, we discuss its epidemiological and ecological implications.

2. DATA SET AND BASIC EPIDEMIC PATTERNS

(a) *Data set*

We focus on weekly measles notifications in 60 towns and cities in England and Wales. These are official notifications, taken from the Registrar General's Weekly Reports—more details of the data set are given by Keeling & Grenfell (1997). The clearest epidemic dynamics are before the onset of measles vaccination in 1967. We therefore analyse the pre-vaccination data set from the start of 1944 to the end of 1966. Local annual birth rates and population sizes are taken from the Annual Reports of the Registrar General. The observed notifications are corrected for a 60% rate of under-reporting (Clarkson & Fine 1985).

(b) *Epidemiological patterns*

In this section, we describe the observed patterns in the spatiotemporal data set. These are then analysed by the statistical models described in the next section.

Figure 1a shows the aggregate time-series of notifications for the 60 cities. It reflects the well-known tendency, in developed countries before vaccination, for large-scale biennial measles epidemics, superimposed on smaller seasonal variations in incidence (Bartlett 1957; Fine & Clarkson 1982; Anderson *et al.* 1984; Schenzle 1984). The set of sample autocorrelation plots (ACF) for selected cities in figure 1b–h illustrates that large centres, such as London, tend to have regular epidemics, while smaller towns below the CCS (such as King's Lynn) have more irregular patterns. Bartlett (1957) categorized regular (type I and II) epidemics in large and medium cities, giving way to irregular (type III) patterns in small centres, especially when the latter are geographically isolated.

We can characterize these patterns in more detail by considering individual epidemic waves. Figure 2 shows the weekly pre-vaccination time-series for a selection of cities. Following the school year, each series is split into a sequence of fixed two-year segments from October (week 1 in the graphs) to the end of September (week 104 in the graphs). Each segment therefore displays a two-year-cycle with the major epidemic in the first year and the minor epidemic in the second year of the cycle. Figure 2 displays the 11 epidemic waves from 1944 to 1966 plotted on top of each other. The thick line indicates the sequence of median points which constitutes an image of the expected epidemic wave.

The overall biennial pattern has been described in detail by Fine & Clarkson (1982). The main epidemic

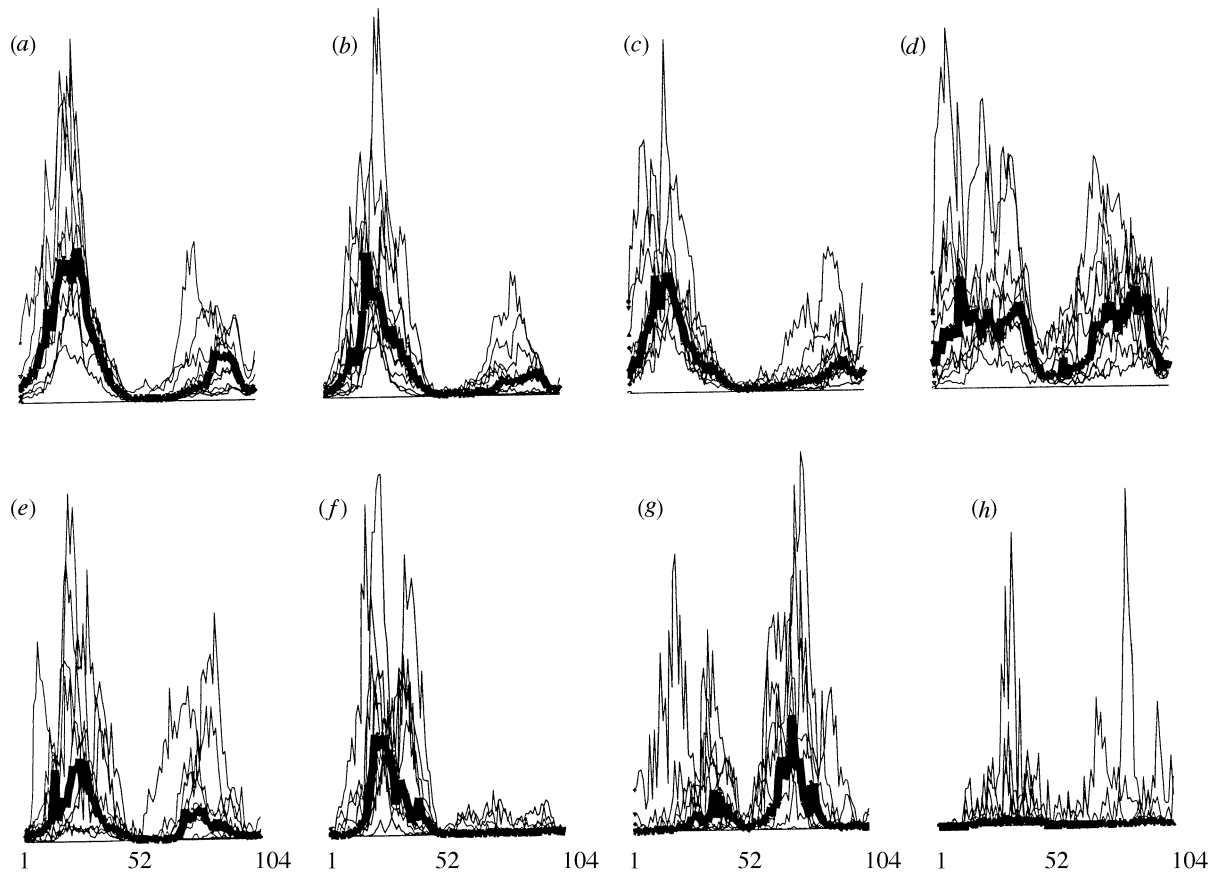


Figure 2. Plot of the 11 biennial waves for a selection of cities. Weeks 1–52 constitute the major epidemic year for most cities. Weeks 53–104 are referred to as the minor epidemic year. The thick line indicates the median wave. (a) London; (b) Birmingham; (c) Manchester; (d) Liverpool; (e) Coventry; (f) Plymouth; (g) Norwich; (h) King's Lynn.

outbreak starts in early October, approximately a month after the start of the school term and lasts until July, reaching its peak value in late February or early March. It is followed by a long trough during summer, which ends when the school term starts in autumn, leading to a minor epidemic outbreak during spring term of the following year. The latter is followed by a short decrease until the next main epidemic occurs. We will refer to the first year as the *major epidemic* and the second as the *minor epidemic year*.

Figure 2 reveals a number of local patterns, superimposed on the average picture. The two-year pattern, with major epidemics in odd years, is fairly synchronous among the cities in the sample. A significant exception to this is Norwich, which has major epidemics in even years during the 1950s. We return to Norwich's exceptional behaviour in the discussion. Apart from Norwich, the correlation coefficient between each town and the average pattern for other centres is relatively high, even for remote towns. Figure 3 shows a histogram of the estimated correlation coefficients. Small communities have more sudden and violent eruptions compared to large and medium sized cities like London, Birmingham, Manchester, or Leeds (figure 2). In the latter, we see similar endemic two-year patterns with periodic main epidemics and minor seasonal outbreaks.

Liverpool is unusual among large communities in that successive major and minor epidemics were of almost

the same height during the 1940s and 1950s. This distinction has been attributed to Liverpool's relatively high birth rate—and resultant quick replacement of susceptibles after major epidemics (Grenfell *et al.* 1994*a,b*, 1995*a*). This pattern is also seen in other towns with high birth rates, such as Birkenhead, Coventry, Newcastle and Sunderland. All these centres have large minor epidemics, usually in conjunction with lesser peaked previous major epidemics. The impact of the minor epidemic de-emphasizes the biennial pattern in Liverpool's autocorrelation function (figure 1*e*).

In contrast, communities such as Plymouth (figure 2), as well as Southampton, Brighton, Bolton, Wolverhampton, Derby, Walsall, and Reading, have longer periods of extinction during the second year and hence show a clear-cut two-year pattern. It is therefore not so much the shape of the main epidemic but the pattern of intervening minor epidemics which varies among the cities. For example the striking difference between Liverpool and Manchester in figures 1 and 2 illustrates that even geographically close communities of similar population sizes may have a completely different pattern during the minor epidemic year.

In the following section, we derive a GLM to account for these variations in terms of local differences in recruitment of susceptibles, driven by heterogeneities in birth rate, and regional spatial heterogeneity, measured by the degree of isolation of individual towns and cities.

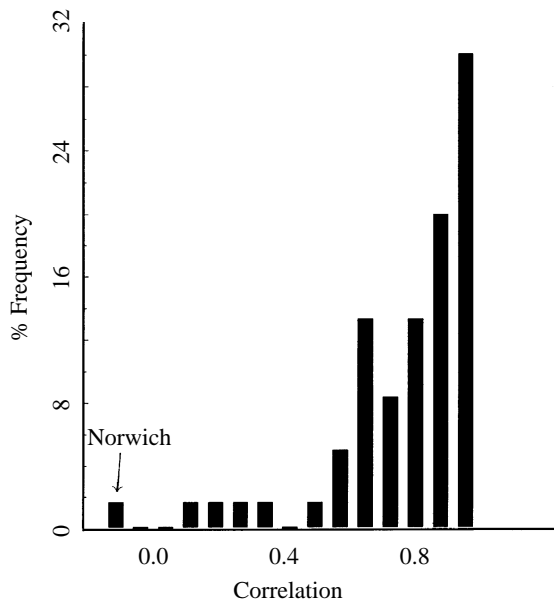


Figure 3. Frequency distribution of the ordinary sample correlation coefficient between the yearly counts of cases of each city and the average over the remaining 59 cities. The average correlation is 0.73 indicating a high degree of synchronicity. This also means that even remote cities may have a large correlation with each other. For instance Sheffield and Plymouth have a correlation of 0.89 even though they are separated by about 370 km. Norwich is the only city having a negative correlation (-0.15). Some small cities such as King's Lynn (0.20), Great Yarmouth (0.10), or Exeter (0.26) are only weakly correlated with the average because of their irregular pattern.

3. STATISTICAL MODELS

We start by estimating a GLM that relates the number of cases during the whole of a two-year segment to demographic and neighbourhood variables. Next, we model the main epidemic and the minor epidemic years as well as the pattern of local extinctions of infection separately.

Regional patterns of epidemiological coupling in measles have been a topic of much work in spatial geography (Murray & Cliff 1975; Cliff *et al.* 1981, 1993). However, direct measures of the (mainly childhood) movement patterns which underlie disease spread are generally only available from small-scale studies (Sattenspiel & Dietz 1995). Here, we therefore investigate a range of indirect measures of epidemiological isolation, based on the matrix of geographical distances and measures of regional population density. These measures are described in more detail below.

Consider the following probability model. Let $y_{i,w}$ denote the response variable, for instance the counts of infected or the counts of fadeouts in city i ($i = 1, \dots, 60$) during wave w ($w = 1, \dots, 11$). Let $P_{i,w} = \beta' \mathbf{x}_{i,w}$ denote a continuous predictor function linear in β , where $\mathbf{x}_{i,w}$ is a vector of explanatory variables and a constant for the intercept. We assume that the $y_{i,w}$ are realizations from a random variable Y . In the GLM the expected value of the response variable Y is assumed to be influenced by the stimulus variables through the linear predictor function:

$$E(Y|\mathbf{x}_{i,w}) = g(\beta' \mathbf{x}_{i,w}) = g(P_{i,w}) \quad (1)$$

or equivalently

$$P_{i,w} = g^{-1}(E(Y|\mathbf{x}_i)) \quad (2)$$

where g^{-1} is the link function (see McCullagh & Nelder 1989).

(a) Explanatory variables

Vector $\mathbf{x}_{i,w}$ consists of the following candidate covariates.

$B_{i,w}$: the birth rate of community i at the time of wave w . The data are recorded on a yearly basis. Before vaccination, measles infection was strongly associated with the pattern of schooling (Fine & Clarkson 1982). We therefore consider lagged birth rates (up to a lag of five years before the middle year of wave w), to allow for delayed recruitment to the school-susceptible cohort. The corresponding covariates are denoted by B_1, \dots, B_5 .

$Pop_{i,w}$: the population size of community i at the time of wave w (yearly records). Since we are looking at absolute counts of cases we expect a proportional dependence on the population size under the null hypothesis.

Neighbourhood covariates: we consider the following variables as representations of different assumptions about geographical and neighbourhood effects.

Regional density of towns, ND_i : the average distance in km of community i to the next b neighbouring cities in the sample set. Preliminary correlation analyses suggested that we take three neighbours.

Regional population density, $NP_{i,w}$: the sum of population sizes (at the time of wave w) of the communities in the sample set that are within a given geographical distance of community i .

Regional density of cases, $NI_{i,w}$: the sum of infected individuals (in wave w) of the communities in the sample set that are within a given geographical distance of community i . Preliminary correlation analyses suggested that we take a radius of 16 km for NP and NI .

Hierarchical regional density of cases, $NIH_{i,w}$: prompted by Cliff *et al.*'s (1993) work on measles diffusion, we also considered the following hierarchical measure of potential transmission. Let $S_{i,w}(b)$ denote the set of b cities that are nearest in distance to i and for which the population size is larger than $Pop_{i,w}$. Define

$$NIH_{i,w}(b) = \sum_{j \in S_{i,w}(b)} a_{ij} c_{j,w},$$

where

$$a_{ij} = \frac{e^{-d_{ij}}}{\sum_{l \in S_{i,w}(b)} e^{-d_{il}}}$$

are exponential weights of the distance d_{ij} from site i to j , $c_{j,w}$ is the number of cases in city j during the minor epidemic time of wave w . Each larger neighbour in the set is thus weighted exponentially according to its distance to city i such that the closest larger town is of largest importance. NIH therefore accounts for hierarchical transmission from large to smaller centres according to

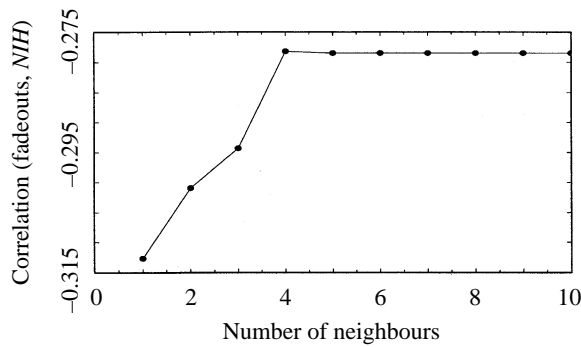


Figure 4. Correlation between the number of fadeouts and number of cases during the minor epidemic year in the neighbouring b larger towns (NIH on a log scale) against number of neighbours b . The largest negative correlation is at $b=1$ so that we used the next largest neighbour for the estimation.

the geographical distance. For London, which does not have larger neighbours, we defined $NIH_{i,w} = c_{i,w}$ since there are enough infected individuals during trough time to sustain the epidemics. Figure 4 shows the negative correlation between the number of fadeouts and $NIH_{i,w}(b)$ against b . This is largest for $b = 1$ so that we used the next largest neighbour for the estimations.

All explanatory variables are transformed onto a logarithmic scale. In order for the response variable to be regressed on up to a five-year delayed birth rate the regressions cover the time-span from 1948 to 1966 (waves 3–11). Hence, there are 540 data points spanning nine waves and 60 cities.

(b) Dependent variables

(i) *Modelling absolute counts of disease incidence*

To study the conditional mean of model (1), assumptions have to be made about the parametric form of the density of Y and the link function. The data display substantial extra variation relative to a Poisson model for counts of cases. We therefore choose the negative binomial distribution, as a contagious Poisson distribution which can accommodate overdispersion due to intersite variability observed here (McCullagh & Nelder 1989). The mean and variance of the negative binomial distribution are given by

$$E(Y|x) = \mu, \quad \text{Var}(Y|x) = \mu + \frac{\mu^2}{k}, \quad (3)$$

where the parameter k is estimated as an inverse measure of the degree of overdispersion relative to the Poisson. Figure 5 shows a plot of the mean of the response variable (overall two-year wave) against the estimated variance for the different cities. Clearly, the variance is larger than the mean and approximately follows the functional relationship given in (3) for $k = 12$.

In order to fit the GLM given in (1) to the count data, the parameters β are estimated by maximum likelihood, using the logarithmic link function. See Lawless (1987) for a detailed treatment of the negative binomial regression and the derivation of the likelihood function. We made use of an s -plus function for likelihood estimation provided by Venables & Ripley (1994). In fitting the

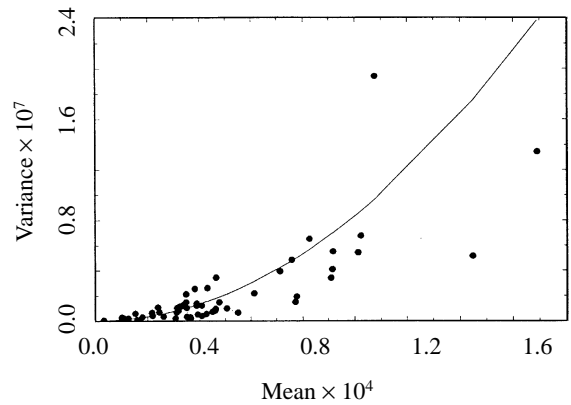


Figure 5. Variance versus mean of the number of cases (biennial cycle) estimated separately for each city.

models by maximum likelihood, we implicitly assume spatial and temporal independence of epidemics. Though there is likely to be some dependence, we believe the assumption is reasonable as a first approximation. The selection of a parsimonious subset of covariates was based on the t -values of the coefficients. As a measure of goodness-of-fit we give the squared Pearson correlation coefficient, r^2 , between the observed data and the model predictions (Mittelböck & Schemper 1996).

With a logarithmic link equation (1) becomes

$$\log(E(Y_{i,w}|\mathbf{x}_{i,w})) = \beta' \mathbf{x}_{i,w}, \quad (4)$$

where $\mathbf{x}_{i,w}$ denotes the set of the explanatory variables that characterize the local factors and regional coupling of town i during wave w as listed above. $Y_{i,w}$ is the total number of cases in the following time periods during the biennial epidemics:

- model 1; the *overall* two-year wave w ,
 - model 2; the *major* epidemic year of wave w ,
 - model 3; the *minor* epidemic year of wave w ,
- for $w = 3 \dots, 11$ and $i = 1 \dots, 60$.

(ii) *Modelling the pattern of fadeout in epidemic troughs*

In order to correct for notification errors fadeouts are generally defined as three or more successive weeks without cases (Bartlett 1957, 1960). Here, for simplicity, we refer to any zero count as a fadeout. Large cities such as London, Birmingham and Liverpool did not fade out whereas Teignmouth, which is the smallest town in the sample, typically faded out for more than one year during a biennial cycle.

In order to estimate the relationship between the proportion of fadeouts during a two-year wave and the covariates, we assume the following logistic GLM:

$$\text{model 4: } \text{logit}(p_{i,w}) = \log\left(\frac{p_{i,w}}{1 - p_{i,w}}\right) = \beta' \mathbf{x}_{i,w}, \quad (5)$$

where $\mathbf{x}_{i,w}$ is the vector of explanatory variables as defined above, and $p_{i,w}$ is the probability of having a fadeout in city i ($i = 1, \dots, 60$) at wave w ($w = 3, \dots, 11$). The observed proportions of fadeouts in city i during wave w are used as probability estimates.

The s-shaped logistic model is well suited to model the mean, however the residual mean deviance exceeds unity. We can well expect heterogeneity as we are adding across successive fadeouts which are not independent in time. We correct for this extra binomial variation (see Collet 1991) by rescaling the variance parameter using the function supplied in s-plus. Alternatively, one could allow for the overdispersion in the logistic model by using the beta-binomial distribution (see Lindsey 1995).

4. RESULTS

The estimation results for models 1–4 are given in the corresponding tables. Clearly, the number of cases and the fadeout proportion are largely explained by the population size. The slope of this relationship on the log scale is not significantly different from unity. This indicates that, overall, there are no major geographical or temporal variations in notification efficiency. Furthermore, the birth rate at a delay time of four years (B_4) is found to have a positive effect on the number of cases (in models 1 and 3) and a negative effect on the fadeout proportion (model 4). If B_4 is included as a covariate in any of the models, then other delays in the birth rate are not significant and hence are dropped from the regressions. We now consider models 1–4 in detail.

(a) *Model 1 (table 1): overall 2 year-waves*

The residual deviance (p -value 0.304) and the Pearson r^2 indicate a good fit for model 1, including the population size and B_4 as covariates. None of the spatial neighbourhood covariates were found to improve the fit of the model. Figures 6a and 6b show the separate partial effects of the population size and birth rate. Most of the variability is captured by population size, but, additionally, birth rate has a significant positive influence. The partial effects are also discernible in figure 6c which provides a scatterplot of both the model predictions and the observed values against the population size. If the latter were the only significant explanatory variable, then the model predictions would be aligned on a narrow line. The fact that they occupy a broad band is caused by the additional explanatory power of the birth rate.

(b) *Model 2 (table 2): main epidemic years*

The number of cases during the major epidemic years can be explained almost entirely as proportions of the population size. The coefficients for the birth rate and neighbourhood covariates are close to zero. Figure 6d shows a plot of the model predictions against population size. The predictions occupy a narrow line, indicating that none of the other covariates have much explanatory power. The p -value of the residual deviance and the Pearson r^2 measure indicate a good fit for model 2. The data points are slightly more dispersed for smaller towns. This happens because small places may have low counts when they occasionally miss out on a main epidemic.

(c) *Model 3 (table 3): Minor epidemic years*

The estimated measure of dispersion \hat{k} (table 3a) for model 3 shows that the data are more dispersed in the troughs than for the major epidemics (model 2) or the

Table 1. *Results of ML estimation for model 1*

(The upper part gives the estimated coefficients, their standard errors, and t -values. The next line shows the estimated dispersion parameter \hat{k} and its standard error. The null deviance denotes the deviance of the model without covariates (other than a constant). The residual deviance is the deviance of the estimated model. Note that the latter is approximately distributed as χ^2 , hence a p -value > 0.05 indicates a satisfactory fit of the model. The Pearson r^2 is the squared Pearson correlation coefficient between the observed data and the model predictions.)

	coefficients	s.e.	t ratio
constant	−1.024	0.4411	−2.322
population	0.991	0.0159	42.422
birth rate B_4	0.574	0.0863	6.655
dispersion parameter \hat{k}	10.229	0.62	—
deviance null model	5988.894	539 d.f.	—
deviance residuals	553.265	537 d.f.	p -val 0.305
Pearson r^2	0.93	—	—

biennial cycle (model 1). The ML estimation indicates that, in addition to population size, the birth rate B_4 and the neighbourhood covariate NIH have a significant positive effect. A larger minor epidemic in a regional centre therefore generates more cases during the minor epidemic outbreaks in the surrounding smaller towns. However, the estimated residuals are asymmetric, indicating that the negative binomial assumption is not appropriate for the trough data. It is therefore difficult to test for the influence of the covariates during the minor epidemic years.

To overcome this problem, we retain the assumption of a linear relationship in the logs but perform estimation via ordinary least squares, deriving confidence intervals from bootstrap replications of the model (see Efron & Tibshirani 1993, ch. 9). This allows us to draw inferences about the influence of the covariates without imposing parametric assumptions on the distribution. The bootstrap confidence intervals confirm the previous results (see table 3b). Moreover, the least squares estimates give slightly larger importance to the birth rate and the neighbourhood covariate. The estimated residuals are symmetric, indicating that this approach provides a better fit to the trough data than the negative binomial model. Figure 6e shows the predictions of the least squares model. The wide band of predictions demonstrates that the birth rate and neighbourhood effects are important covariates in addition to the population size. The stepwise inclusion of covariates reveals that the birth rate explains 7.6% and NIH an additional 19.36% of the variation that remains if population size was the only covariate.

(d) *Model 4 (table 4): proportion of fadeouts*

The log odds ratio of fadeouts is proportional to the population size as well as the birth rate at delay 4. Cities have less fadeouts if their population size and birth rate are higher. Also the neighbourhood covariates, in particular NIH , have explanatory power. However, if NIH is included in the regression, then the other spatial covariates are not significant and can therefore be dropped.

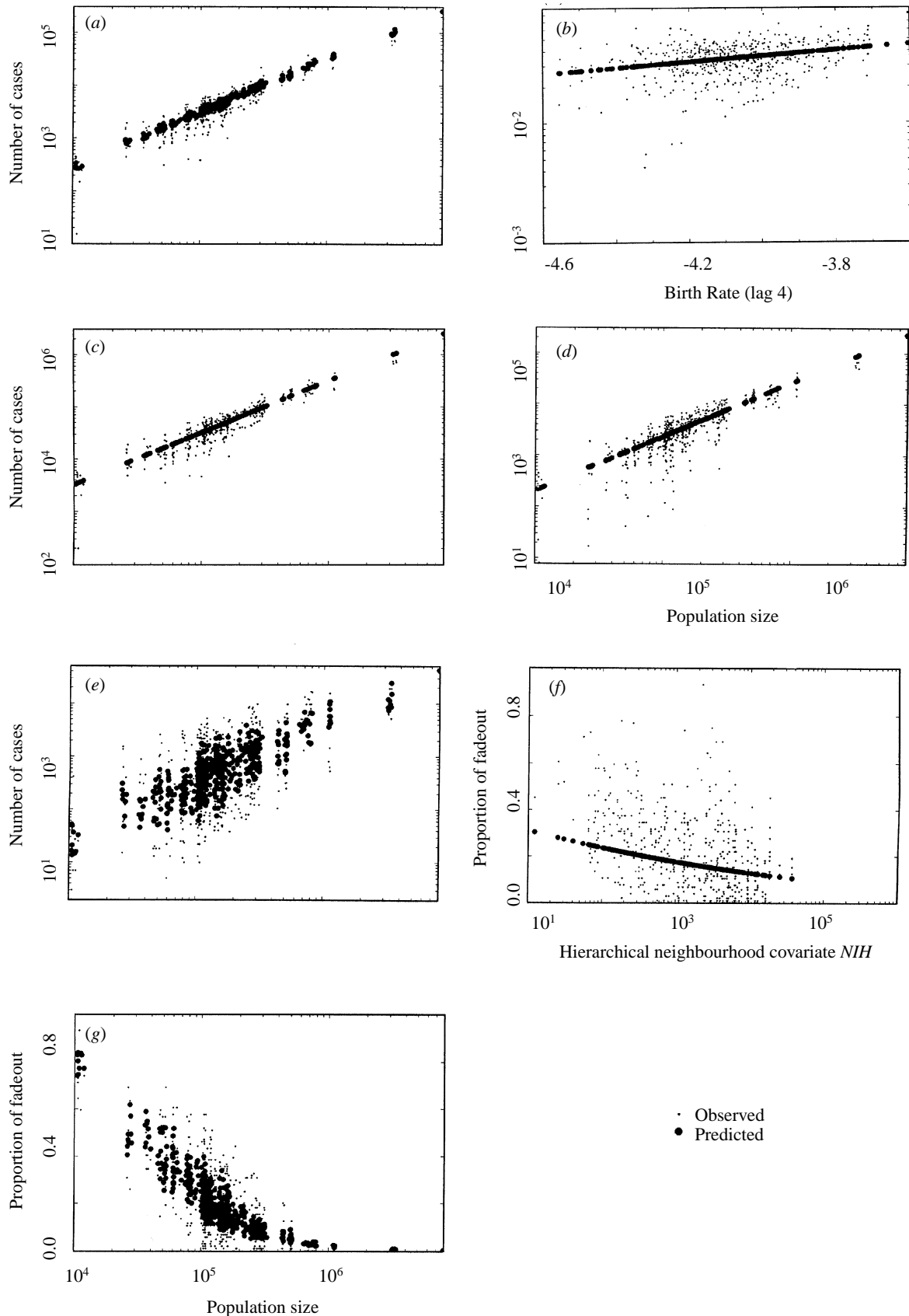


Figure 6. Graphical results for models 1–4 (see tables 1–4 for the parameter estimates). Predictions from the estimated models are indicated by large points and observed values are denoted by small points. (a) and (b) Model 1: partial effects (other variables held constant) of the population size and the birth rate at lag 4. (c) plot of overall model predictions and the observed values against the population size for model 1. Graphs (d), (e) and (g) give the same plot for models 2, 3, and 4, respectively. The predictions have a wide spread in (e) and (g) indicating that the birth rate and the neighbourhood covariate explain more of the additional variation in models 3 and 4 than in model 2 (graph (d)). (f) Plot of the predicted negative partial effect of *NIH* on the proportions of fadeouts.

Table 2. *Results of ML estimation for model 2*

(The notation is the same as in table 1.)

	coefficients	s.e.	<i>t</i> ratio
constant	-3.861	0.7212	-5.353
population	1.039	0.0259	40.059
birth rate B_4	0.084	0.1410	0.599
dispersion parameter \hat{k}	3.819	0.225	—
deviance null model	2658.28	539 d.f.	—
deviance residuals	566	537 d.f.	<i>p</i> -val 0.187
Pearson r^2	0.89	—	—

Table 3. *Estimation results for model 3*

((a) Results for the ML estimation under the negative binomial assumption. The *p*-value indicates a poor fit. Moreover, the residuals are asymmetric with a mean different from zero. (b) Results for the LS estimation where 90% confidence intervals are derived from 300 bootstrap replications of the model. Note that none of the confidence intervals contain zero. The LS residuals are symmetric around zero.)

(a) ML estimation	coefficients	s.e.	<i>t</i> ratio
constant	2.773	1.500	1.849
population	0.745	0.056	13.303
birth rate B_4	1.562	0.295	5.297
<i>NIH</i>	0.219	0.030	7.246
dispersion parameter \hat{k}	0.908	0.048	—
deviance null model	1149.15	539 d.f.	—
deviance residuals	629.62	537 d.f.	<i>p</i> -val 0.004
Pearson r^2	0.86	—	—
(b) least squares fit			(90% conf)
constant	1.413		(-1.182, 3.739)
population	0.776		(0.667, 0.886)
birth rate B_4	1.728		(1.171, 2.205)
<i>NIH</i>	0.358		(0.302, 0.416)
standard deviation	1.191		(1.123, 1.240)
Pearson r^2	0.85		—

This result indicates that large minor epidemics in a regional major centre decrease the chance of local extinction of the disease in the surrounding smaller towns. The negative partial effect of the *NIH* can be seen in figure 6*f*. Figure 6*g* displays a plot of the predicted and observed values against population size. As with model 3, the model predictions have a wide spread, showing that the birth rate and the neighbourhood effects have a significant input. Moreover, the stepwise inclusion of covariates shows that the neighbourhood variable captures more (12.55%) of the remaining variation than the birth rate (5.7%). The *p*-value and the Pearson r^2 indicate a good performance of the logistic model.

5. DISCUSSION

This analysis reveals a balance between local and global influences on population dynamics, which depends on local dynamic state. During major epidemic peaks, only

Table 4. *ML estimation results for model 4*

(See table 1 for the notation. In order to account for the overdispersion in the logistic model, standard errors and deviance are rescaled by the overdispersion factor (see Collett 1991).)

	coefficients	s.e.	<i>t</i> ratio
constant	7.224	1.097	6.586
population	-0.954	0.047	-20.469
birth rate B_4	-0.910	0.205	-4.431
neighbourhood <i>NIH</i>	-0.161	0.020	-8.144
scaling overdispersion	7.510	—	—
deviance null model	1475.62	539 d.f.	—
deviance residuals	577.26	537 d.f.	<i>p</i> -val 0.105
Pearson r^2	0.80	—	—

local population size influences the absolute number of cases—epidemic size as a proportion of population size stays relatively constant. Major epidemics occur when susceptible density rises above a deterministic threshold (Anderson & May 1991). Our results indicate that the local deterministic epidemic dynamics then predominate over the impact of birth rates and geographical coupling.

By contrast, the intervening minor epidemics—and associated fadeouts of infection—are affected both by birth rates and regional geographical structure. These associations are especially strong for the number of fadeouts. Since these are subsumed in the overall counts of cases in the minor epidemics, they could in principle be driving all the dependency on the covariates. However, further analyses (not documented here), which standardize counts by the period of positive notifications, also reveal associations with birth rate and geography.

All the models indicate that the strongest influence of birth rate is at a lag of four years before the middle year of the wave. This reflects the importance of schooling to the dynamics of measles epidemics. The most violent epidemics were in 5–6-year-old children, in their first or second year at primary school (Fine & Clarkson 1982). The four-year lagged birth rate appears to reflect recruitment to these cohorts. In fact, lag 5 birth rates are almost as important as lag 4—however, the autocorrelation between successive birth rates causes the model algorithm to keep the latter in the most parsimonious model. Obviously, other lags are also likely to be influential here—future work should adopt a cohort-based model, estimating how the proportion of susceptibles at different ages is affected by birth rate variations.

Returning to our opening question, we can use the model fits to explore the relative importance of (intrinsic) birth rate and (extrinsic) spatial coupling on the pattern of fadeouts. Stepwise inclusion of these factors indicates clearly that coupling is a much stronger influence on the pattern of fadeouts. This is not surprising, since: (i) birth rates varied over a much narrower range (coefficient of variation in B_4 was 0.162) than our best-fit measure of coupling (coefficient of variation in *NIH* was 1.39); (ii) fadeouts are ended by importation of new cases. They therefore depend directly on the spatial flux of infection, and only indirectly on small (and relatively slowly

changing) variations in the recruitment of susceptibles caused by the birth rate heterogeneities.

Given the absence of explicit information on movement of infectives, we represent spatial variations in infection using relatively crude measures of regional population and case density. There is a universe of such measures and the ones we choose span only some of the possible models for epidemiological coupling. However, it is interesting that a simple hierarchical measure (*NIH*) provides the best association with infection dynamics. This indicates an especially clear analogy with the dynamics of core-satellite metapopulations (Hanski *et al.* 1996).

A much more dramatic example of spatial heterogeneity is provided by Norwich, where major measles epidemics were out of phase with the other cities during much of the 1950s. Given biennial dynamics, it could be that Norwich happened to drift into even year epidemics, independent of its spatial position. However, this seems unlikely, given that whooping cough epidemics in Norwich are also distinct from the national average (D. Earn, personal communication). In terms of the statistical model, Norwich fits the overall epidemic waves (model 1) and fadeout pattern (model 4) reasonably well. However, (not surprisingly) it is an outlier in the comparative peak and trough analyses (models 2 and 3, respectively) during its period of asynchrony.

We are currently amassing a much more detailed spatiotemporal data set, which will allow a more refined analysis, both of the incidence of dynamic outliers, such as Norwich, and of the best metric to characterise epidemiological diffusion in general. Analyses of spatial diffusion of epidemics (Cliff *et al.* 1993)—particularly in the hinterland between out-of-phase centres—should be especially useful here.

Overall, the cross-sectional GLM with negative binomial errors provides a successful tool for teasing out proximate influences on the epidemic sequence. The associated dispersion measure, \hat{k} , indicates more variation in the minor epidemic model, which fits the negative binomial assumption less well than the peak and biennial wave models. There may be scope here for a more mechanistic maximum likelihood approach, which characterizes the extra variation in the troughs in terms of demographic stochasticity.

Though this analysis does not examine longitudinal measles dynamics explicitly, it does give us pointers about the underlying dynamical system. In particular, model 1 indicates that each biennial sequence accounts for roughly the same number of cases, allowing for longitudinal variations in birth rate. This implies a density-dependent trade-off between successive major and minor epidemics. A comparison of such patterns with the dynamics of current measles models will be the subject of a future paper.

We have focused on the dynamics of measles before vaccination. Obviously, a much more significant applied issue is the balance between recruitment and spatial coupling during the vaccine era. This is an important area for future work, though the analysis is likely to be much more complex. Specifically, we cannot estimate the importance of local variations in susceptible recruitment without spatiotemporal data on variations in vaccine uptake.

In conclusion, this work provides a picture of the balance between local and regional influences on the dynamics of measles metapopulations. It also illustrates

the potential of epidemiological data for addressing general questions in population dynamics.

This work was supported by the Wellcome Trust (B.F. and B.G.) and the Royal Society (B.G.). The authors thank Ottar N. Bjørnstad, Neal Alexander, and Matt Keeling for various helpful comments.

REFERENCES

- Allen, J. C., Schaffer, W. M. & Rosko, D. 1993 Chaos reduces species extinction by amplifying local population noise. *Nature* **364**, 229–232.
- Anderson, R. M. & May, R. M. 1991 *Infectious diseases of humans: dynamics and control*. Oxford University Press.
- Anderson, R. M., Grenfell, B. T. & May, R. M. 1984 Oscillatory fluctuations in the incidence of infectious disease and the impact of vaccination: time series analysis. *J. Hyg.* **93**, 587–608.
- Bartlett, M. S. 1957 Measles periodicity and community size. *J. R. Statist. Soc. A* **120**, 48–70.
- Bartlett, M. S. 1960 The critical community size for measles in the US. *J. R. Statist. Soc. A* **123**, 37–44.
- Bjørnstad, O. N., Champely, S., Stenseth, N. C. & Saitoh, T. 1996 Cyclicity and stability of grey-sided voles, *Clethrionomys rufocanus*, of Hokkaido—spectral and principal components analyses. *Phil. Trans. R. Soc. London B* **351**, 867–875.
- Bjørnstad, O. N., Falck, W. & Stenseth, N. C. 1995 A geographic gradient in small rodent density fluctuations—a statistical modelling approach. *Proc. R. Soc. London B* **262**, 127–133.
- Bolker, B. M. & Grenfell, B. T. 1995 Space, persistence and the dynamics of measles epidemics. *Phil. Trans. R. Soc. London B* **348**, 309–320.
- Bolker, B. M. & Grenfell, B. T. 1996 Impact of vaccination on the spatial correlation and dynamics of measles epidemics. *Proc. Nat. Acad. Sci. USA* **93**, 12 648–12 653.
- Clarkson, J. A. & Fine, P. E. M. 1985 The efficiency of measles and pertussis notification in England and Wales. *Int. J. Epidemiol.* **14**, 153–168.
- Cliff, A. D., Haggett, P., Ord, J. K. & Versey, G. R. 1981 *Spatial diffusion: an historical geography of epidemics in an island community*. Cambridge University Press.
- Cliff, A. D., Haggett, P. & Smallman-Raynor, M. 1993 *Measles: an historical geography of a major human viral disease from global expansion to local retreat, 1840–1990*. Oxford: Blackwell.
- Collet, D. 1991 *Modelling Binary Data*. London: Chapman & Hall.
- Dietz, K. & Schenzle, D. 1985 Mathematical models for infectious disease statistics. In *A celebration of statistics* (ed. A. C. Atkinson & S. E. Feinberg), pp. 167–204. New York: Springer.
- Efron, B. & Tibshirani, R. J. 1993 *An introduction to the bootstrap*. London: Chapman & Hall.
- Ferguson, N. M., Anderson, R. M. & May, R. M. 1997 Scale, persistence and synchronicity: measles as a paradigm of a spatially-structured ecosystem. In *Spatial ecology: the role of space in population dynamics and interspecific interactions* (ed. D. Tilman & P. Kareiva). Princeton, NJ: Princeton University Press.
- Fine, P. E. M. & Clarkson, J. A. 1982 Measles in England and Wales. I. an analysis of factors underlying seasonal patterns. *Int. J. Epidemiol.* **11**, 5–15.
- Gilpin, M. & Hanski, I. 1991 *Metapopulation Dynamics: Empirical and Theoretical Investigations*. London: Academic Press.
- Grenfell, B. T. 1992 Chance and chaos in measles dynamics. *J. R. Statist. Soc. B* **54**, 383–398.
- Grenfell, B. T., Bolker, B. M. & Kleczkowski, A. 1995a Demography, seasonality and the dynamics of measles in developed countries. In *Epidemic models: their structure and relation to data* (ed. D. Mollison), pp. 248–270. Cambridge University Press.

- Grenfell, B. T., Bolker, B. M. & Kleczkowski, A. 1995*b* Seasonality and extinction in chaotic metapopulations. *Proc. R. Soc. London B* **259**, 97–103.
- Grenfell, B. T. & Harwood, J. 1997 (Meta)population dynamics of infectious diseases. *Trends Ecol. Evol.* **12**, 395–399.
- Grenfell, B. T., Kleczkowski, A., Ellner, S. P. & Bolker, B. 1994*a* Non-linear forecasting and chaos in ecology and epidemiology: measles as a case study. In *Chaos and forecasting* (ed. H. Tong), pp. 321–345. Singapore: World Scientific.
- Grenfell, B. T., Kleczkowski, A., Ellner, S. P. & Bolker, B. M. 1994*b* Measles as a case-study in nonlinear forecasting and chaos. *Phil. Trans. R. Soc. London A* **348**, 515–530.
- Grenfell, B. T., Kleczkowski, A., Gilligan, C. A. & Bolker, B. M. 1995*c* Spatial heterogeneity, nonlinear dynamics and chaos in infectious diseases. *Statist. Meth. Med. R.* **4**, 160–183.
- Hanski, I., Moilanen, A. & Gyllenberg, M. 1996 Minimum viable metapopulation size. *Am. Nat.* **147**, 527–541.
- Hanski, I., Poyry, J., Pakkala, T. & Kuussaari, M. 1995 Multiple equilibria in metapopulation dynamics. *Nature* **377**, 618–621.
- Hassell, M. P., Comins, H. N. & May, R. M. 1991 Spatial structure and chaos in insect population dynamics. *Nature* **353**, 255–258.
- Hill, J. K., Thomas, C. D. & Lewis, O. T. 1996 Effects of habitat patch size and isolation on dispersal by *Hesperia comma* butterflies: implications for metapopulation structure. *J. Anim. Ecol.* **65**, 725–735.
- Holt, R. D. 1994 Ecology at the mesoscale: the influence of regional processes on local communities. In *Species diversity in ecological communities* (ed. R. E. Ricklefs & D. Schluter), pp. 77–88. Chicago and London: University of Chicago Press.
- Keeling, M. J. & Grenfell, B. T. 1997 Disease extinction and community size: modeling the persistence of measles. *Science* **275**, 65–67.
- Kuussaari, M., Nieminen, M. & Hanski, I. 1996 An experimental study of migration in the Glanville fritillary butterfly *Melitaea cinxia*. *J. Anim. Ecol.* **65**, 791–801.
- Lawton, J. H., Nee, S., Letcher, A. J. & Harvey, P. H. 1994 Animal distributions: patterns and processes. In *Large-scale ecology and conservation biology* (ed. P. J. Edwards, R. M. May & N. R. Webb), pp. 41–58. Oxford: Blackwell.
- Lawless, J. F. 1987 Negative binomial and mixed Poisson regression. *Can. J. Statist.* **15**, 209–225.
- Levins, R. 1969 Some demographic consequences of environmental heterogeneity for biological control. *Bull. Entomol. Soc. Am.* **15**, 237–240.
- Lindsey, J. K. 1995 *Modelling frequency and count data*. Oxford: Clarendon Press.
- May, R. M. & Anderson, R. M. 1984 Spatial heterogeneity and the design of immunization programs. *Math. Biosci.* **72**, 83–111.
- McCullagh, P. & Nelder, J. A. 1989 *Generalized linear models* 2nd edn. London: Chapman & Hall.
- Mittelböck, M. & Schemper, M. 1996 Explained variation for logistic regression. *Statist. Med.* **15**, 1987–97.
- Murray, G. D. & Cliff, A. D. 1975 A stochastic model for measles epidemics in a multi-region setting. *Inst. Br. Geogr.* **2**, 158–174.
- Nee, S. 1994 How populations persist. *Nature* **367**, 123–124.
- Olsen, L. F., Truty, G. L. & Schaffer, W. M. 1988 Oscillations and chaos in epidemics: a nonlinear dynamic study of six childhood diseases in Copenhagen, Denmark. *Theor. Popul. Biol.* **33**, 344–370.
- Ranta, E., Kaitala, V., Lindstrom, J. & Helle, E. 1997 The Moran effect and synchrony in population dynamics. *Oikos* **78**, 136–142.
- Ruxton, G. D. 1994 Low levels of immigration between chaotic populations can reduce system extinctions by inducing asynchronous regular cycles. *Proc. R. Soc. London B* **256**, 189–193.
- Sattenspiel, L. & Dietz, K. 1995 A structured epidemic model incorporating geographic mobility among regions. *Math. Biosci.* **128**, 71–91.
- Schaffer, W. M. & Kot, M. 1985 Nearly one dimensional dynamics in an epidemic. *J. Theor. Biol.* **112**, 403–427.
- Schenzle, D. 1984 An age-structured model of pre- and post-vaccination measles transmission. *IMA J. Math. Appl. Med. Biol.* **1**, 169–191.
- Sutcliffe, O. L., Thomas, C. D. & Moss, D. 1996 Spatial synchrony and asynchrony in butterfly population dynamics. *J. Anim. Ecol.* **65**, 85–95.
- Sutcliffe, O. L., Thomas, C. D. & Peggie, D. 1997*a* Area-dependent migration by ringlet butterflies generates a mixture of patchy population and metapopulation attributes. *Oecologia* **109**, 229–234.
- Sutcliffe, O. L., Thomas, C. D., Yates, T. J. & Greatorex-Davies, J. N. 1997*b* Correlated extinctions, colonizations and population fluctuations in a highly connected ringlet butterfly metapopulation. *Oecologia* **109**, 235–241.
- Venables, W. N. & Ripley, B. D. 1994 *Modern applied statistics with S-plus*. Statistics and Computing. Berlin, Heidelberg, New York: Springer.

As this paper exceeds the maximum length normally permitted, the authors have agreed to contribute towards production costs.